

Non-isolated resonant quasi-Z-source network DC–DC converter

M. Adamowicz[✉]

A novel non-isolated resonant quasi-Z-source network DC–DC converter is proposed. The resonant impedance source network is derived from the quasi-Z-source network by including the autotransformer-based resonant cell instead of the second inductor of the quasi-Z-network. The leakage inductance of the autotransformer and two resonant capacitors connected in series with the autotransformer windings constitute a high-frequency resonant tank. At the same time, the resonant operation with a sinusoidal current of the main switch and diodes enables electromagnetic interference mitigation and improves the efficiency of the converter. Experimental results of a 100 W, 30 V/200 V prototype are presented to verify the analysis results of the proposed converter.

Introduction: A quasi-impedance source (quasi-Z-source) network converter presents an interesting alternative to the conventional boost converter offering wide voltage conversion with continuous input current and load short-circuit protection. The quasi-Z-source DC–DC converter, shown in Fig. 1a includes quasi-Z-network with the input diode and four energy storage elements: two inductors and two capacitors. Although the quasi-Z-source converter can have theoretically infinite voltage gain, its boost factor is affected by series resistances of the inductors and the forward voltage drop of the input diode. Various techniques have been applied to the quasi-Z-source converter to improve its voltage gain. In [1], a step-up DC–DC converter has been proposed which combines voltage multiplier cells to the secondary winding of the coupled inductor which was included in the second inductor of the quasi-Z-source network. In [2], the A-source network has been proposed, in which the secondary inductor of the quasi-Z-source network is replaced with an autotransformer for realising a very high DC voltage gain. Unfortunately, a high turns ratio of the autotransformer increases the di/dt of the main switch, which may cause several electromagnetic interference problems. Moreover, at higher power, the DC flowing through the A-source autotransformer windings tends to saturate the core.

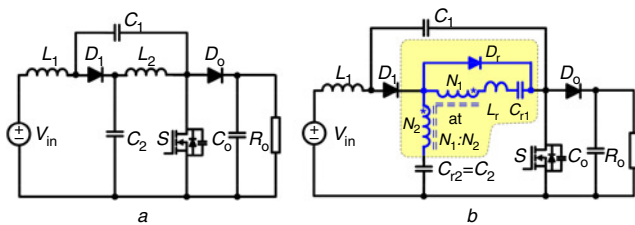


Fig. 1 Quasi-Z-source network DC–DC converter

a Basic topology
b Conceptual converter with autotransformer-based resonant cell

The conceptual non-isolated resonant quasi-Z-source network DC–DC converter proposed in the present Letter is shown in Fig. 1b. The high-DC voltage gain with the resonant operation and sinusoidal current of the main switch is achieved by replacing the second inductor (L_2) of the quasi-Z-network with $L_r C_r D_r$ resonant cell and including $N_1:N_2$ autotransformer to couple the $L_r C_r D_r$ cell with the second capacitor (C_2) of the quasi-Z-network. The capacitor C_2 in the same way plays the role of the second resonant capacitor C_{r2} . Theoretical analysis and experimental results are provided to verify the validity of the proposed converter.

System configuration: Fig. 2 shows the proposed converter and its key waveforms. The high-frequency autotransformer is modelled as a magnetising inductor L_m , an ideal transformer with turns ratio $1:n$ and a primary leakage inductor L_{Lk} . The zero current switching (ZCS) of the input diode D_1 and the resonant diode D_r is realised by resonance between the resonant capacitors C_{rp} and C_{rs} , connected in parallel, and the autotransformer leakage inductance L_{Lk} . The resonant capacitors C_{rp} and C_{rs} at the same time block the DC-bias current of the autotransformer.

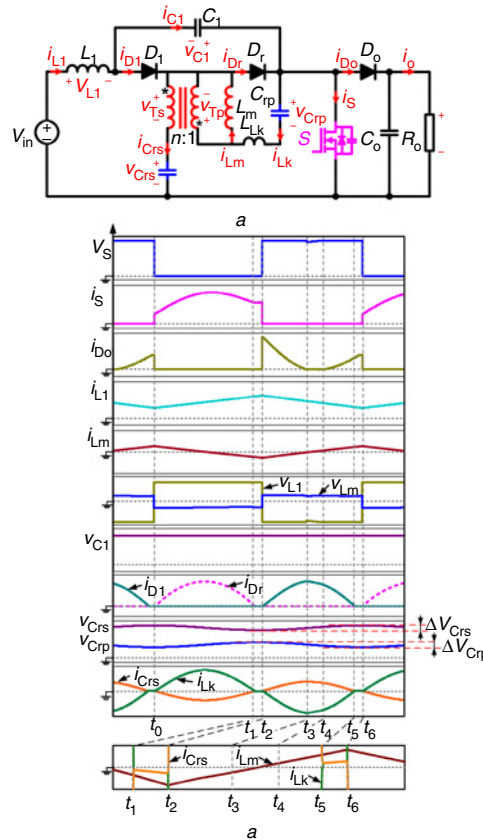


Fig. 2 Proposed converter and its key waveforms

Basic operating principles: For the sake of simplicity all components of the analysed converter are assumed ideal. The output voltage equals the voltage of the main switch during turn off which is the sum of the input voltage V_{in} and voltages of capacitor C_1 and inductor L_1

$$v_S(t) = V_{in} - v_{L1}(t) + v_{C1}(t), \quad (1)$$

where

$$-v_{L1}(t) = (n+1)v_{Lm}(t) + L_{Lk} \frac{di_{Lk}(t)}{dt}. \quad (2)$$

The operating modes of the proposed converter are essentially divided into five modes shown in Fig. 3.

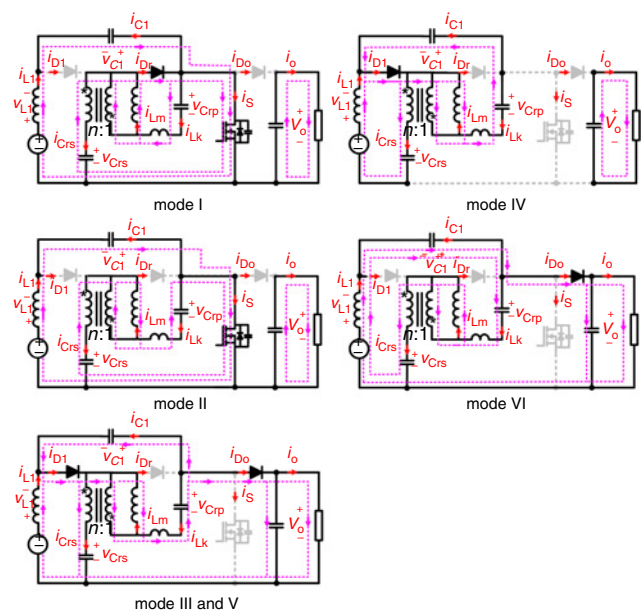


Fig. 3 Operational mode diagrams

Mode 1 [$t_0 \sim t_1$]: At time t_0 , the main switch S is turned on. The input diode D_1 is reverse biased and the energy previously stored in C_1 is transferred to the inductor L_1 . The output diode D_o is reverse biased and the load R_o is supplied by the capacitor C_o . The resonant diode D_r is forward biased and two resonance capacitors C_{rp} and C_{rs} and the leakage inductor L_{Lk} begin to resonant

$$i_{Lk}(t) = \left(\frac{v_{CrS}(t_0)}{nL_{Lk}} - \frac{v_{CrP}(t_0)}{L_{Lk}} \right) \frac{1}{\omega} \sin \omega(t - t_0), \quad (3)$$

where $\omega = 1/\sqrt{L_{Lk}C_r}$ and $C_r = \sqrt{C_{rp}n^2C_{rs}/(C_{rp} + n^2C_{rs})}$.

Mode 2 [$t_1 \sim t_2$]: At the beginning of this time interval the resonance between L_{Lk} and resonant capacitors C_{rp} and C_{rs} is finished and diode D_r is turned off at ZCS condition. The voltage v_{CrP} reaches its maximum value and v_{CrS} reaches its minimum value. The currents flowing through autotransformer primary and secondary have both negative values, close to zero and are equal which results from the finite permeability of the autotransformer core and non-zero reluctance of the autotransformer magnetic circuit. Switch S is still turned on and the input inductor current i_{L1} is further increased due to the charging action of capacitor C_1 .

Mode 3 [$t_2 \sim t_3$]: At time t_2 , switch S turns off and, then, the input diode D_1 and the output rectifier D_o is turned on to deliver the input energy to the output load through the autotransformer. Part of another input inductor energy transfers to impedance source capacitor C_1

Mode 4 [$t_3 \sim t_4$]: At time t_3 diode D_o turns off naturally at zero current, i_{L1} flows through the autotransformer and charges the impedance source capacitor C_1 .

Mode 5 [$t_4 \sim t_5$]: As diode D_o conducts, part of the input energy flows through D_o . In this mode, diode D_1 continues to turn on to provide the current flowing path for i_{L1} until C_1 is completely charged accordingly to (6), diode D_1 is then turned off with ZCS.

Mode 6 [$t_5 \sim t_6$]: This time interval begins when diode D_1 is turned off at ZCS condition and C_1 starts to discharge to load. The voltage v_{CrS} reaches its maximum value and v_{CrP} reaches its minimum value. The autotransformer primary and secondary currents have positive values close to zero and are equal, which is the effect of the non-zero reluctance of the autotransformer magnetic circuit. This time interval ends when the switch S is turned on again.

Applying the volt-second law to the input inductor L_1 and the magnetizing inductor L_m

$$\int_{t_0}^{DT+t_0} v_{L1}(t)dt + \int_{DT+t_0}^{T+t_0} v_{L1}(t)dt = 0, \quad (4)$$

$$\int_{t_0}^{DT+t_0} v_{Lm}(t)dt + \int_{DT+t_0}^{T+t_0} v_{Lm}(t)dt = 0, \quad (5)$$

following equations for the input capacitor voltage V_{C1} and average voltages of the resonant capacitors $V_{CrP-avg}$ and $V_{CrS-avg}$ can be written

$$V_{C1} = (1/(1-D))V_{CrP-avg} = (1/(n(1-D)))V_{CrS-avg}, \quad (6)$$

where D represents the duty cycle of main switch S . Consequently, the voltage gain of the proposed DC-DC converter can be obtained as

$$M = \frac{V_o}{V_{in}} = \frac{1 + (1/n)}{1 - \frac{n+1}{n}D}. \quad (7)$$

Experimental results: A 100 W prototype with 200 V/0.5 A output and 100 kHz switching frequency was implemented in the laboratory to verify the analysis results of the proposed converter. The input voltage (V_{in}) is 35 V. The resonant capacitors C_{rp} and C_{rs} are 2 and 1 μ F, respectively. The 0.2 mH input inductor (L_1) is implemented with the T225-26B-type toroid core. The $n = 1.8$ autotransformer using low-loss F867-type core has magnetising inductance $L_m = 1.6$ mH and the primary leakage inductance $L_{Lk} = 1.5$ μ H. The duty ratio of main switch S is $D = 0.5$. Experimental results for the output voltage (V_o), the main switch voltage (v_s) and currents of the resonant diode (i_{Dr})

and the input diode (i_{D1}) are depicted in Fig. 4a. Owing to the resonance between L_{Lk} and capacitors C_{rp} and C_{rs} , the input diode D_1 is switched at ZCS condition which minimises the diode overall loss. The resonant capacitors currents i_{CrP} and i_{CrS} in Fig. 4b correspond to the currents of the primary and secondary winding of the autotransformer.

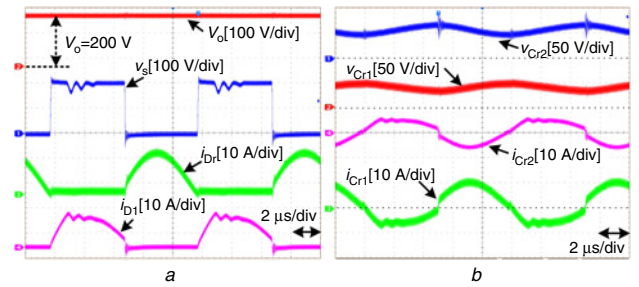


Fig. 4 Experimental results

a Output voltage V_o , voltage of switch v_s and diode currents i_{D1} and i_{Dr}
b Resonant capacitors C_{rp} and C_{rs} , voltages v_{CrP} , v_{CrS} and currents i_{CrP} , i_{CrS}

Fig. 5 shows the voltage gain with the variation of turns ratio n and duty cycle D and the measured efficiency of the proposed converter.

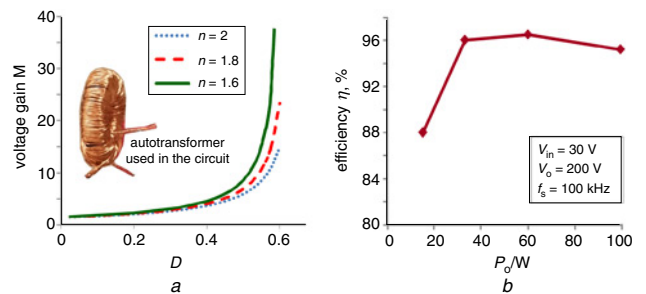


Fig. 5 Voltage gain and efficiency (experimental results)

Conclusion: A novel autotransformer-based non-isolated resonant quasi-Z-source network DC-DC converter is proposed in the Letter. The used autotransformer turns ratio enables the high voltage gain of the converter. Owing to resonance between autotransformer leakage inductance and resonant capacitors connected in series with the transformer windings the ZCS operation of diode D_1 of the quasi-Z-network can be achieved. This feature alleviates the reverse recovery problem of the diode meanwhile reduces turn off loss of the diode. The capacitors connected in series with the autotransformer windings prevent the core from saturation and allow the reduction of size and weight of the autotransformer and the whole converter. Owing to the resonant operation of the main switch the reduction of its di/dt can be also achieved

© The Institution of Engineering and Technology 2019

Submitted: 17 April 2019 E-first: 11 June 2019

doi: 10.1049/el.2019.1311

One or more of the Figures in this Letter are available in colour online.

M. Adamowicz (Gdansk University of Technology, Narutowicza Str.11/12, 80-233 Gdansk, Poland)

✉ E-mail: marek.adamowicz@pg.edu.pl

References

- Andrade, A.M.S.S., and Guisso, R.A.: 'Quasi-Z-source network DC-DC converter with different techniques to achieve a high voltage gain', *Electron. Lett.*, 2018, **54**, (11), pp. 710-712, doi: 10.1049/el.2018.1005
- Ayachit, A., Siwakoti, Y.P., Galigekere, V.P.N., et al.: 'Steady-state and small-signal analysis of A-source converter', *Trans. Power Electron.*, 2018, **33**, (8), pp. 7118-7131, doi: 10.1109/TPEL.2017.2756626